Theriogenology 118 (2018) 233–242

Contents lists available at ScienceDirect

Theriogenology

journal homepage: www.theriojournal.com

Cumulus cells of camel (*Camelus dromedarius*) antral follicles are multipotent stem cells

Islam M. Saadeldin [a, c, *, 1], Ayman Abdel-Aziz Swelum [a, d, 1], Mona Elsafadi [b], Amer Mahmood [b], Musaad Alfayez [b, e], Abdullah N. Alowaimer [a]

[a] Department of Animal Production, College of Food and Agricultural Sciences, King Saud University, 11451, Riyadh, Saudi Arabia
[b] Stem Cell Unit, Department of Anatomy, College of Medicine, King Saud University, Riyadh, Saudi Arabia
[c] Department of Physiology, Faculty of Veterinary Medicine, Zagazig University, 44519, Zagazig, Egypt
[d] Department of Theriogenology, Faculty of Veterinary Medicine, Zagazig University, 44519, Zagazig, Egypt
[e] Saudi Society for Camel Studies, Saudi Arabia

ARTICLE INFO

Article history:
Received 15 January 2018
Received in revised form
14 May 2018
Accepted 17 June 2018
Available online 19 June 2018

Keywords:
Cumulus cells
Differentiation
Ovary
Multipotent stem cells
Camel

ABSTRACT

The mammalian ovary is a highly dynamic organ, in which proliferation and differentiation occur constantly during the entire life span, particularly in camels that are characterized by a follicular wave pattern and induced ovulation. Granulosa cells are the main cells of mature follicles. Two distinct cell types, namely, the mural and cumulus granulosa cells are distinguished on the basis of antral fluid increase. The multipotency of follicular fluid and the luteinizing cell were recently demonstrated. However, reports regarding the plasticity of cumulus cells are lacking. We obtained cumulus cells from cumulus-oocyte complexes and showed that camel cumulus cells expressed stem cell mRNA transcripts (*POU5A1*, *KLF4*, *SOX2*, and *MYC*) and were able to differentiate into other non-ovarian follicular cell types *in vitro*, such as neurons, osteoblasts, and adipocytes. In contrast, removal of the ooplasm (oocytectemy) showed no effect on cumulus cell proliferation and differentiation. This is the first report to identify an invaluable source of multipotent stem cells, which is routinely discarded during *in vitro* embryo production. The plasticity and transdifferentiation capability of camel cumulus cells definitely requires attention as it provides a cheap biological experimental model for basic research in stem cells and for understanding ovarian differentiation, both of which are relevant for use in regenerative medicine and tissue engineering in humans and animals.

1. Introduction

The Arabian camel (*Camelus dromedarius*) is a unique species and is a better provider of meat and milk in desert areas than other farm animals, which are severely affected by the heat and scarcity of food and water in the desert [1]. Camels occupy a special niche in the Arabian agricultural system. The total population of dromedary is estimated to be about 25 million heads all over the world [2].

Camel racing is a highly profitable and well-organized sport, and considered an important traditional and animal agribusiness activity in the Arabian Gulf states. Fractures are the major injuries incurred during racing; however, camel orthopedics is poorly understood because camels are nervous animals, which hinders comprehensive studies on fracture healing [3]. Furthermore, principles of bovine and equine orthopedics cannot be applied to camels orthopedics in absolute terms [4]. Therefore, a basic understanding of bone repair is essential to save the lives camels used in this agribusiness. The bone tissue engineering concept is a relatively new method for repairing damaged bones and involves the regeneration of tissues using stem cells, scaffolds, and growth factors, with stem cells playing a leading role in tissue repair and regeneration [5–7].

Only two reported studies covered camel stem cell research, and thus this field is still in its infancy [8,9]. Recently, for the first time, we isolated embryonic stem-like cells from camel embryos under feeder-free conditions that expressed all genes associated with pluripotency (*POU5A1* or *OCT4*, *SOX2*, *KLF4*, and *MYC*) [9].

The adult mammalian ovary is a highly dynamic organ, in which

* Corresponding author. Department of Animal Production, College of Food and Agricultural Sciences, King Saud University. 11451, Riyadh, Saudi Arabia.
E-mail address: isaadeldin@ksu.edu.sa (I.M. Saadeldin).
[1] Equally contributed authors.

https://doi.org/10.1016/j.theriogenology.2018.06.009
0093-691X/

proliferation and differentiation occur constantly, e.g. during follicular waves. Interestingly, studies have examined the multipotency of follicular granulosa cells and showed the plasticity of the follicular granulosa cells and they were multipotent and can differentiate *in vitro* into neurogenic, osteogenic, chondrogenic, hepatocytic, adipogenic cells, and muscular filaments [10–19]. In addition, studies have reported some ovarian diseases are associated with metaplasia of the ovarian tissue, such as transdifferentiation of ovarian cells into osetoblasts [20–22] and into adipocytes [23,24].

Therefore, this study aimed to examine the multipotency and plasticity of camel cumulus cells. This will offer an easy and cheap cost-effective source of multipotent camel stem cells and would provide a model to study ovarian diseases caused by transdifferentiation and metaplasia.

2. Methods

2.1. Chemicals

Hormones and chemicals were obtained from Sigma-Aldrich Corp. (St. Louis, MO, USA) unless otherwise stated.

2.2. Cumulus-oocyte complexes recovery

Camel ovaries (n = 130) were obtained from a local abattoir and transported in 0.9% (v/v) NaCl solution at 30–33 °C to the laboratory within 3–4 h of slaughter. The follicular contents of antral follicles (2–6 mm in diameter) were aspirated using an 18-gauge needle attached to a 10 ml-disposable syringe. Cumulus-oocyte complexes (COCs) with evenly granulated cytoplasm that were enclosed by more than three layers of compact cumulus cells were selected and washed thrice with HEPES-buffered tissue culture medium-199 (TCM-199) supplemented with 2 mM $NaHCO_3$, 10% (v/v) fetal bovine serum (FBS), and 50 μg/mL gentamycin sulfate [25,26].

2.3. Experimental design

COCs were randomly selected and cultured to permit cumulus cells attachment. Oocytes were gently stripped from the attached cumulus cells after 24 h and the culture medium was then changed every 2 days until confluence. Cells were used to generate embryoid body-like spheroids and then were examined for targeted differentiation into adipocyte, osteocyte and neurons through supplementing the culture medium with specific differentiation factors. In order to examine whether the oocytes affect the plasticity of the cumulus cells, ooplasm was aspirated and cumulus cells were examined to differentiate into neurons. Biological and technical replicates were considered in every experimental procedure.

2.4. Cumulus cell culture

Primary cumulus cell culture was performed using COCs (n = 20/well, 5 replicates) on four-well polystyrene-coated tissue culture dishes (Falcon, BD Biosciences, Franklin lakes, NJ, USA) for 24 h at 38 °C in a humidified atmosphere of 5% CO_2. The culture medium was Dulbecco's modified Eagle's medium (DMEM-F12) supplemented with 5% FBS, 0.1 mM β-mercaptoethanol, 1% nonessential amino acids, 2 mM L-glutamine, 10 ng/mL EGF, 10 ng/mL fibroblast growth factor-2 (FGF-2, Miltenyi Biotec. GmbH, Bergisch Gladbach, Germany), 1% insulin-transferrin-selenium, and 1 mg/mL gentamycin [9]. Oocytes were stripped gently using a glass micropipette (160 μm internal diameter) from the attached cumulus cells and discarded. Cumulus-granulosa cells were maintained in culture for 2 days and the medium was changed every 2 days until confluence was reached.

2.5. Quantitative polymerase chain reaction

mRNA levels of cumulus cells were compared to those of embryonic stem-like (ES-like) cells previously isolated in our laboratory [9]. Cumulus cells (20 COCs, three replicates) were pelleted after washing with phosphate buffered saline (PBS) and used for total an RNA extraction Kit (iNtRON Biotechnology, Inc., Daegu, South Korea) according to the manufacturer's instructions. RNA concentration and purity were estimated using a NanoDrop 2000 spectrophotometer (Thermo Fisher) by calculating the ratios of absorbance at 230, 260, and 280 nm; samples showing values of A260/A280 of $\geq$2.0 and A260/A230 > 2.0 were used for reverse transcription (RT). Pulsed RT was used to increase complementary DNA (cDNA) transcription efficiency [27] as follows; 120 cycles of 16 °C for 2 min, 37 °C for 1 min, and 50 °C for 0.1 s, followed by a final inactivation at 85 °C for 5 min. Individual RT reactions were performed using a SuperScript™ III First Strand Synthesis System (Thermo Fisher) according to the manufacturer's instructions. Total RNA (50 ng) and random hexamers were used in a 40-μL reaction volume according to the manufacturer's instructions. Relative quantification of mRNA expression was determined by real-time PCR (ViiA™7, Applied Biosystems, Foster City, CA, USA). Reactions contained 100 ng cDNA, 1 μM each of the forward and reverse primers, and 1X SYBR Green premix (Applied Biosystems) were run in triplicates. Following normalization to the mRNA levels of the reference gene *GAPDH*, fold-change and relative quantification of *POU5A1, SOX2, KLF4, MYC,* and *NANOG* transcripts was performed using the $2^{-\Delta\Delta Ct}$ method [28]. In all assays, cDNA template-negative and reactions without RT showed negative amplification. The expression of ES-like cells was set as an arbitrary control to calculate the fold-change for different transcripts. The thermal cycler conditions were 95 °C for 10 min, followed by 40 cycles of 95 °C for 10 s, 60 °C for 20 s, and 72 °C for 40 s. Primer sequences, annealing temperature, and approximate product size are listed in Supplemental Table 1. The melting curve for primers was evaluated using theViiATM7 apparatus-associated software.

2.6. Embryoid body-like (EB) formation

At confluence, the cumulus-granulosa cells of the five replicates were harvested and used to form EBs according to a previous method [29]. To form self-aggregated EBs, the cumulus-granulosa cells were mechanically dissociated and allowed to clump into poly-HEMA coated petri dishes and incubated overnight at 38 °C in a humidified atmosphere containing 5% CO_2. On the second day, EB-like structures of various sizes were formed. Individual EBs were collected using a glass micropipette and placed under the various differentiation conditions.

2.7. In vitro adipocyte differentiation

EBs (n = 25, 5 replicates) were cultured in DMEM supplemented with adipogenic induction mixture [30] containing 10% FBS, 10% horse serum, 1% penicillin-streptomycin, 100 nM dexamethasone, 0.45 mM isobutyl methyl xanthine, 3 μg/ml insulin, and 1 μM rosiglitazone (Novo Nordisk, Bagsvaerd, Denmark). The culture medium was replaced after every two days. Cells cultured in standard culture medium were considered as the negative control.

2.8. In vitro osteoblast differentiation

EBs (n = 25, 5 replicates) were cultured in DMEM supplemented

with osteoblast induction mixture [31] containing 10% FBS, 1% penicillin-streptomycin, 50 μg/ml L-ascorbic acid (Wako Chemicals, Neuss, Germany), 10 mM β-glycerophosphate, 10 nM calcitriol (1α, 25-dihydroxyvitamin D3), and 10 nM dexamethasone. The medium was replaced after every two days. Cells cultured in standard culture medium were considered as the negative control.

2.9. In vitro neuronal differentiation

Neuronal differentiation was induced by treatment of EBs (n = 25, 5 replicates) with 10 μM all-trans retinoic acid (R2625, Sigma) using serum-free DMEM-F12 [32] for 6 days with medium change after every 2 days. Cells cultured in serum-free DMEM-F12 plain culture medium were considered as the negative control.

2.10. Cytochemical analysis

2.10.1. Nile Red fluorescence determination and quantification of mature adipocytes

Cells were fixed using 4% paraformaldehyde for 15 min at room temperature, followed by washing with PBS. Nile Red stock solution was prepared (1 mg/ml) in dimethyl sulfoxide (DMSO) and stored at −20 °C away from light. The dye was added directly to the cells (5 μg/ml in PBS) and the cells were incubated for 10 min at room temperature. Fluorescent signal was measured using a SpectraMax/M5 fluorescence spectrophotometer plate reader (Molecular Devices Co., Sunnyvale, CA) in the bottom well-scan mode where nine readings were taken per well using 485 nm for excitation and 572 nm for emission spectra [30].

2.10.2. Oil Red-O staining for lipid droplets

Accumulated cytoplasmic lipid droplets were visualized by staining with Oil Red-O in cells 14 days after supplementation of adipogenic induction media. In brief, after washing cells grown in 24-well plates with PBS, the cells were fixed in 4% formaldehyde for 10 min at room temperature and then rinsed once with 3% isopropanol and stained for 1 h with filtered Oil Red-O staining solution at room temperature (0.5 g Oil Red-O powder in 60% isopropanol w/v). The cells were washed with PBS and visualized under an inverted microscope.

2.10.3. Alizarin Red S (ARS) staining for detection of mineralized matrix

Fourteen-day-old differentiated cells in 24-well plates were

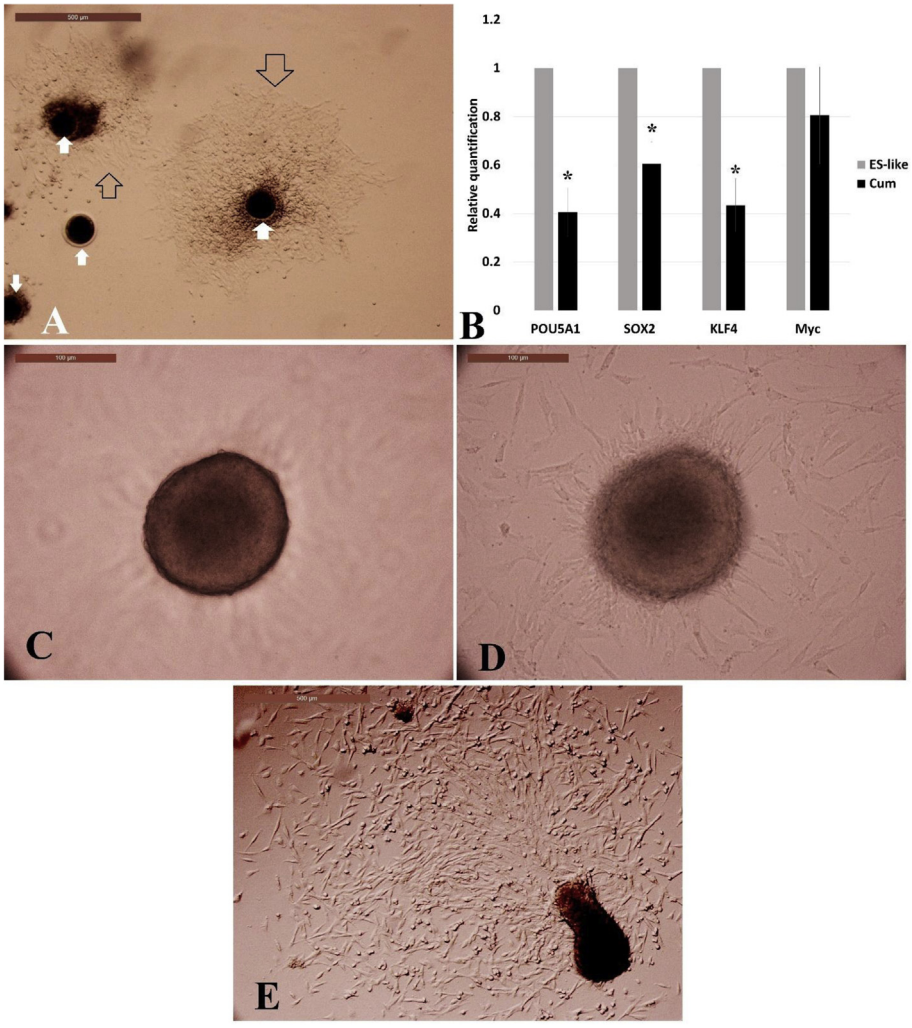

Fig. 1. Primary culture of camel cumulus. a. Cumulus-oocyte complexes were cultured and cumulus cells attached to the culture dish and formed outgrowths (empty black arrows) after 24 h (white arrows indicate oocytes which have been stripped from cumulus cells after 24 h of the culture). b. RT-PCR analysis showing expression of pluripotency markers (*POU5A1*, *SOX2*, *KLF4,* and *MYC*) (asterisks indicate significant differences), except for *MYC*. c. Embryoid body-like spheroids (EBs) formation after mechanical splitting and subculture in low-attachment dishes. d-e. Embryoid body outgrowths observed on day 2 and day 5 of culture, respectively.

washed with PBS and then fixed with 70% ice-cold ethanol for 1 h at −20 °C. The cell layer was rinsed with distilled water and stained with 40 nM ARS (Sigma) pH 4.2 for 10 min at room temperature. Excess dye was washed off with water followed by a wash with PBS for few minutes to minimize nonspecific ARS stain. The cells were then visualized under an inverted microscope.

2.11. Immunofluorescence for neurogenic markers (vimentin, β-tubilin III, and MAP2)

Six days after the addition of retinoic acid, cells were fixed in 4% paraformaldehyde (w/v) in PBS, pH 7.4, for 20 min at room temperature. After washing in PBS, the cells were permeabilized by incubation in PBS containing 0.1% Triton-X100 and blocked by 1% goat serum (Vector Laboratories, Burlingame, CA) for 1 h at room temperature. Dilutions of primary antibodies (1:500 dilution) (mouse mono-clonal) directed against vimentin (#BD-550513, BD Biosciences, San Jose, CA, USA), β-tubilin III (TUJ-1, #ab14545, Abcam, Cambridge, United Kingdom), and MAP2 (HM-2, #ab11267, Abcam) were prepared in antibody diluent solution. Cells were incubated in primary antibody solution for 1 h at room temperature, washed in PBS, then incubated with the secondary antibody (FITC-conjugated goat anti-mouse IgG) (Jackson ImmunoResearch lab. Inc. PA) diluted 1:500 in PBS for 1 h at room temperature before washing with PBS. Cell nuclei were counterstained with 4′, 6′-diamidino-2-phenylindole (DAPI) (Vector Lab. Inc., CA). Cumulus cells not treated with retinoic acid were used as negative controls and cells not treated with the primary antibodies were used as the technical negative control.

2.12. Immunohistochemistry for a neurological marker (SOX2)

After serum blocking, cells were incubated in primary antibody solution for 1 h at room temperature. Dilutions of primary antibody (1:200) (goat poly-clonal) directed against SOX2 (#AF2018, R&D Systems, Minneapolis, MN, USA) were prepared in antibody diluent solution. After incubation, cells were washed in PBS, then incubated in biotinylated secondary antibody (rabbit anti-goat IgG (H + L)-HRP conjugate) (#1721034, Bio-Rad Lab. Hercules, CA, USA) for 30 min. The cells were then incubated in DAB solution for 10 min, followed by washing in PBS. Positive brown reactions were visualized using an inverted light microscope.

2.13. Effect of oocyte on cumulus cells plasticity

COCs were individually distributed into 5 μl drops of handling medium (TCM-199 with 5% FBS) using a micromanipulator (Narishige, Minamishiyama Setagaya-ku, Tokyo, Japan), overlaid with mineral oil, held by holding pipette, and the ooplasmic contents were aspirated using 20-μm (outer diameter) tapered needles. Oocytectomized and control COCs (n = 20 each, 5 replicates) were then washed three times with handling medium and washed in culture medium. Culture medium (previously mentioned) was replaced after every 2 days.

2.14. Single cell colony formation

This assay was performed according to previous studies [33,34] with some modifications. Cumulus cells were shredded into small clumps of few cells (less than ten cells) from the COCs (n = 10, 3

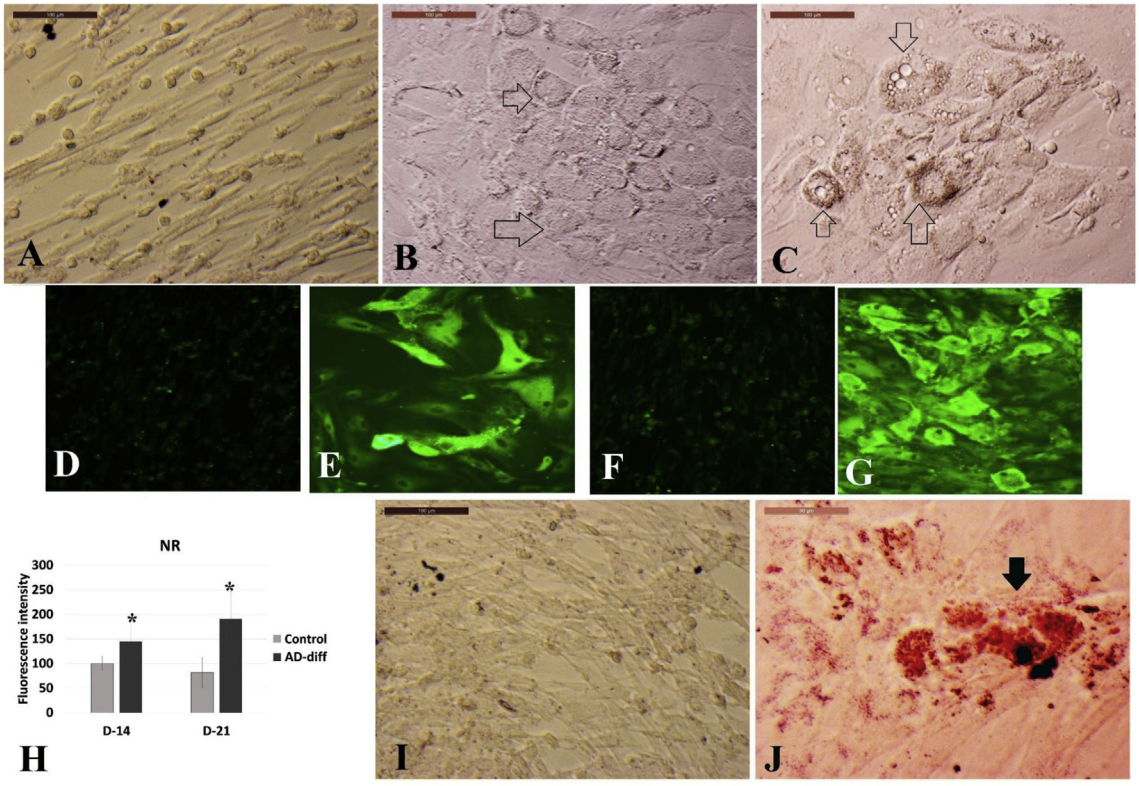

Fig. 2. Targeted differentiation of camel cumulus cells into adipocytes. EBs were differentiated into adipocyte using adipocyte induction medium. a. Control cells were cultured without differentiation factors. b-c. Adipogenic differentiation on days 14 and 21, respectively; cells showed enlarged volume with clear lipid droplet in the cytoplasm (arrows). Nile Red fluorescence under the indicated treatment conditions was performed on days 14 and 21 post-adipocyte induction. Control (d, f) and differentiated (e, g) cells showed comparable fluorescence as presented in histogram (asterisks indicate significant differences, h). Cells were stained on day 21 using Oil Red O staining for adipocytes containing lipid droplets (arrow) and are shown as microscopic images (20×, magnification) for control (i), and adipocytically induced cells (j).

replicates) using two holding pipettes and a micromanipulator, and were then captured with a glass micropipette, seeded into 4-well tissue culture dishes (Falcon), and incubated for 2 days. Culture medium (previously mentioned) was replaced after every 2 days. Doubling time was calculated using an online program (http://www.doubling-time.com/compute.php) by dividing the final and initial cell concentration on day 10 of culture.

2.15. Statistical analysis

Cell proliferation and NR fluorescence were analyzed using Student's t-test. Results of qPCR were analyzed using one-way analysis of variance (ANOVA). $P < 0.05$ was considered statistically significant.

3. Results

3.1. Transcript analysis in camel cumulus cells

Cumulus cells attached to the culture dishes grew rapidly and outgrowths were observed 24 h after the initial culture (Fig. 1a). qPCR analysis showed expression of *POU5A1*, *KLF4*, *MYC*, and *SOX2* mRNA transcripts in cumulus cells compared to embryonic stem-like cells isolated from camel embryos (Fig. 1b). Interestingly, *MYC* expression did not differ between cumulus and ES-like cells.

3.2. Formation of EB-like spheroids

Primary cultured cumulus cells were mechanically passaged and showed formation of EB-like spheroids (EBs) on day 2 of culture in anti-adhesive poly-HEMA coated petri dishes (Fig. 1c). EBs were also able to attach to polystyrene tissue culture dishes and formed out growths (Fig. 1d) and colonies (Fig. 1e).

3.3. Adipogenic differentiation of cumulus cells

Cumulus cell EBs were targetedly differentiated into adipocyte and showed clear morphological differences compared to control cells (Fig. 2) 14 or 21 days after the addition of differentiation factors. Cells became larger in size, cuboidal or polygonal in shape, and contained clearly visible lipid droplets (Fig. 2b and c). Adipogenic differentiation was confirmed by Nile Red fluorescence and showed nearly 1.5-fold and 2-fold increase in fluorescence signals between differentiated and control cells on day 14 and day 21, respectively

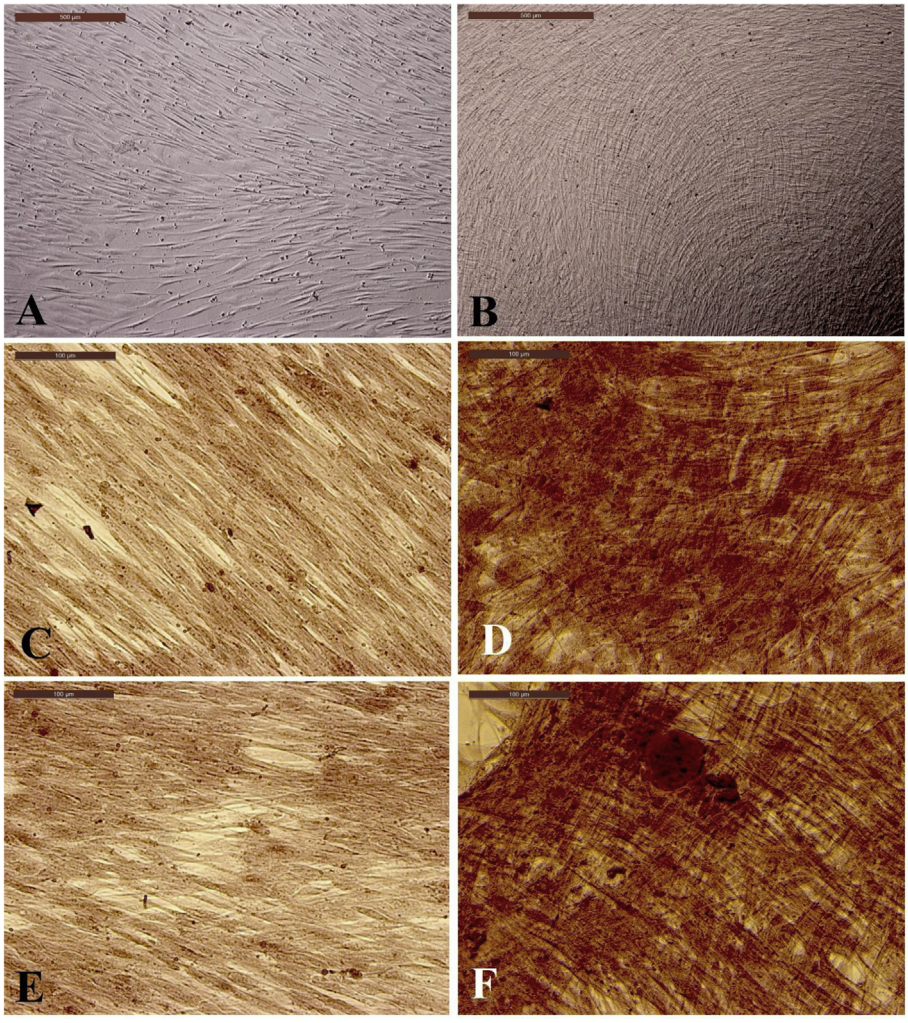

Fig. 3. Targeted differentiation of camel cumulus cells into osteoblasts. EBs were differentiated into osteoblasts (OS) using osteogenic induction mixture for 14 and 21 days. a. Light microscopy images of control (non-induced) and (b) induced EBs on day 21 after induction showed differentiated cells with overlapping or mesh-like arrangement compared with control non-induced cells. c and d show mineralized calcium deposition (throughout the field) after Alizarin Red S staining in control and differentiated cells on day 14, respectively. e and f. Images showing Alizarin staining of control and differentiated cells on day 21, respectively. Note the red staining of mineralization in differentiated cells.

(Fig. 2d–h). Oil Red O staining of differentiated cells showed positive staining of cytoplasmic lipid droplets on day 14 compared to control cells (Fig. 2 i, j).

3.4. Osteogenic differentiation of cumulus cells

Cumulus cell EBs were targetedly differentiated into osteoblasts and showed clear morphological differences with control cells (Fig. 3) 14 or 21 days after the addition of specific differentiation factors. Cells became intercalated and overlapping, showing mesh-like appearance compared to non-differentiated cumulus cells on day 14 of culture (Fig. 3a and b). Calcium and mineralized crystals (red-stained) were clearly visualized via ARS staining of differentiated osteoblasts (Fig. 3c–f).

3.5. Neurogenic differentiation of cumulus cells

Clear morphological changes were observed after culturing cumulus cell EBs in serum-free culture medium supplemented with retinoic acid. Cells showed linear arrangement (Fig. 4a) and some cells showed axon formation or were neuron-shaped or star-shaped. Immunofluorescence analysis showed that the differentiated cells were vimentin- (Fig. 4b), β3-tubulin- (Fig. 4c), and SOX2-positive (Fig. 4d). MAP2 immunofluorescence was observed, but signals were weak in the differentiated cells (Supplemental Fig. 1).

3.6. Spontaneous differentiation

During primary and subsequent passaging of cumulus cells, we observed spontaneous morphological changes in the normal spindle morphology of cumulus cells; at 70% confluence, 50% of the cultured wells (8 wells of total 16) showed different morphology than the typical spindle-shaped cells, such as epithelium-like morphology, axon-like connections, lipid droplet-engorged cells, and fluid filled cyst-like structures (Fig. 5a–d, respectively).

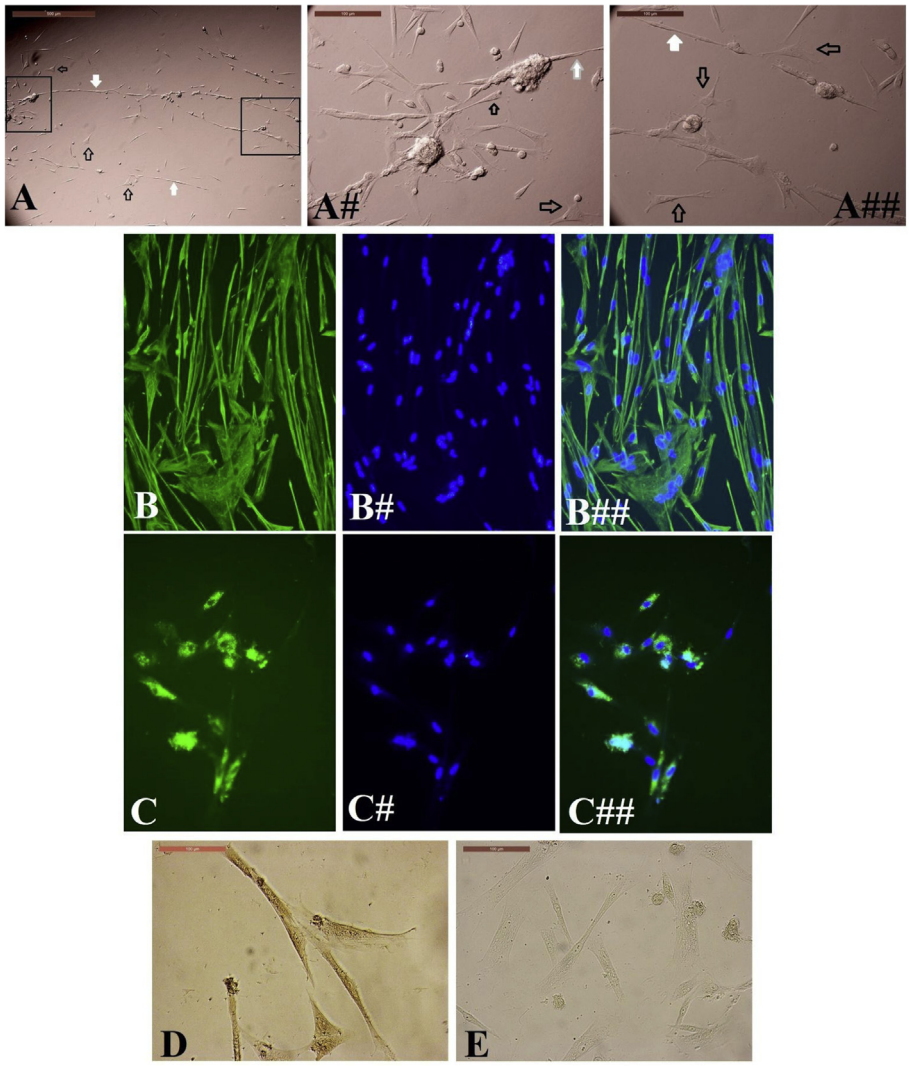

Fig. 4. Targeted differentiation of camel cumulus cells into neurons. EBs were cultured in serum-free medium supplemented with retinoic acid for 6 days. A. Cells showed linear arrangement (white arrows) and some cells showed star-shaped morphology (black arrows). A# and A## represent a higher magnification of (a) showing axon formation (white arrows), neuron-shaped, or star-shaped cells (black arrows). b. B# and B## differentiated cells showing immunofluorescence staining of vimentin, DAPI staining, and merged images, respectively. c. C# and C## represent immunofluorescence staining of β3-tubulin, DAPI staining, and merged images, respectively. d. Immunohistochemical analysis showing the positive DAB reaction (brown color) in differentiated neurons and control (no primary antibodies). Control negative images for immunofluorescence are shown in Supplemental Fig. 1.

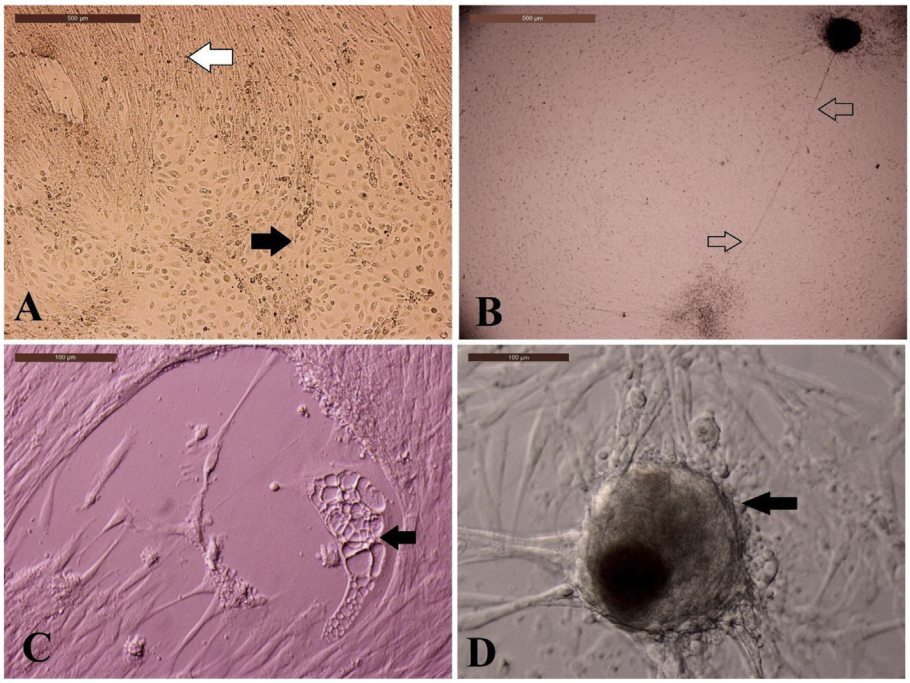

Fig. 5. Spontaneous differentiation of camel cumulus cells. Primary cultured cumulus cells were incubated to continue developing outgrowths in DMEM/F12 culture medium with 10% FBS in 4-well culture dishes and repeated four times (total = 16 wells). At 70% confluence, 50% cells showed morphology different from the typical spindle shaped cells (a, white arrow) such as, epithelial-like morphology (2/16, A. black arrow), axon-like connections (3/16, b, arrows), lipid-engorged cells (1/16, c, arrow), and fluid filled cysts (2/16, d, arrow).

3.7. Effect of oocyte on cumulus cell plasticity

To examine the role of oocytes on cumulus plasticity, ooplasm was aspirated through micromanipulation and oocytoectomized COCs were compared to the controls. There was no difference in cumulus cell attachment and growth or targeted neuronal differentiation between the control and oocytoectomized COC-derived cumulus cells (Fig. 6a–f).

3.8. Single cell proliferation and colony formation

The cumulus cell mass showed rapid growth and colony formation (Fig. 7a and b) and reached confluence after 7 days of culture (mean diameter of the colony = 4.2 ± 0.7 mm), which fully covered the surface area of the 4-well dish on day 10 of culture. Doubling time was 16.02 ± 1.2 h.

4. Discussion

Stem cell research holds promise for regenerative medicine and personalized cell therapy for traumatic, injured, or fractured elite and genetically superior camels used for show, racing, or milking. In this regard, we recently isolated camel embryonic stem-like cells. In this study, we demonstrated that cumulus cells are an easy source of multipotent stem cells that can differentiate into adipocytes, osteoblasts, and neurons, which can be used for regenerative medicine and might provide a model for studying ovarian diseases associated with metaplasia or transdifferentiation.

Cumulus cells expressed mRNAs of genes associated with pluripotency at a level comparable to those of ES-like cells except for *MYC* (Fig. 1B). Reports show that *MYC* activation is associated with increased cell growth [35,36], which might explain the higher doubling time reported in our study (Fig. 6). Moreover, the expression of stem cell markers and the multipotency of granulosa cells were confirmed in human mature ovarian follicular cells by examining the ability to differentiate into neuron-like cells, chondrocytes, adipocytes, hepatocytes, and osteoblasts [10–17]. The expression of different stem cell markers such as *POU*51A, high telomerase activity, and the ability to differentiate into different cell types underline the stem cell characteristics of granulosa cells [13].

Results showed that cumulus cells were able to form embryoid body-like spheroids (EBs), which coincides with those reported in the adult ovarian-derived stem cells [37–40].

Additionally, follicular granulosa cells derived from pig ovary can transdifferentiate into osteoblasts [41]. Moreover, the osteogenic regenerative potential of ovarian granulosa cells was confirmed *in vitro*. These cells also participated in new bone formation *in vivo*, thus confirming their therapeutic and regenerative potential [42]. Our results showed clear morphological differences between the control and differentiated cumulus cells 6 days post-retinoic acid addition (for neuronal differentiation), and 14 days after expression of adipogenic and osteogenic differentiation factors.

Interestingly, cultured granulosa cells derived from human ovarian preovulatory follicles showed certain neurogenic properties, produced acetylcholine, and expressed functional muscarinic acetylcholine receptors, a system speculated to increase proliferation, disrupt gap junctional communication, and alter intracellular calcium levels and the expression of transcription factors [43,44].

The differentiated cells showed neural markers such as vimentin, β3-tubulin, MAP2, and SOX2. Vimentin is often used as a marker of astrocyste or radial glia cells [45,46] and also as a marker for mesenchymally-derived cells or cells undergoing an epithelial-to-mesenchymal transition (EMT) during embryoid development [47]. Additionally, β3-tubulin is a class of tubulin, the expression of which is limited to neurons and is used to label immature neurons [48,49]. Moreover, SOX2 is a transcription factor required for neural plate formation [50]. It is also expressed in proliferating cells and those that acquire glial fates, but is downregulated in post-mitotic neurons [51]. In contrast, microtubule-associated protein 2 (MAP2)

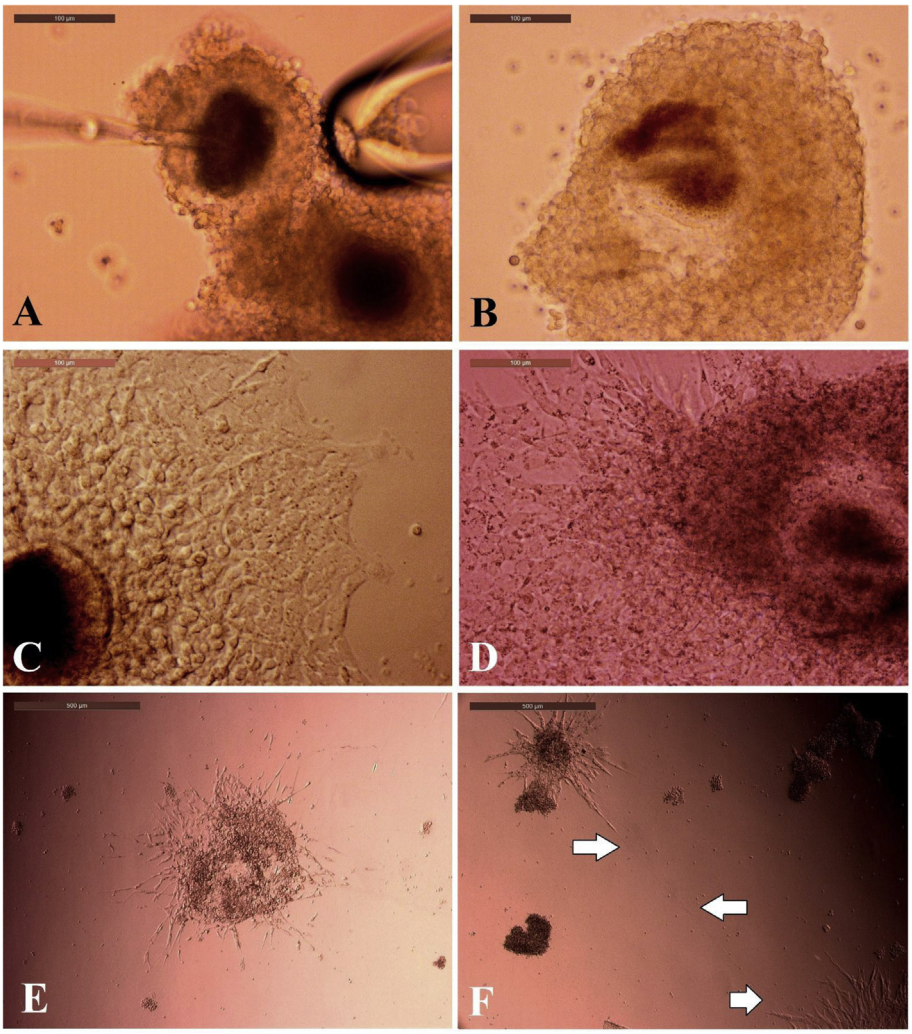

Fig. 6. Effect of oocytes on cumulus cell plasticity. a. The procedure for oocytectomy is presented. b. The oocytectomized COCs are shown. Culture of control (c) and oocytectomized (d) COCs showed normal growth. Subsequent subculture of cumulus cells from control (e) and oocytectomized (f) COCs showed no difference in the ability to form neuron-like projections or shuttle connections between the two colonies (f. arrows, ~1.5 mm length), after retinoic acid supplementation in the medium.

is a neuron-specific protein that promotes assembly and stability of the microtubule network; although its expression is weak in neuronal precursors, the expression increases during neuronal development. Hence, MAP2 is commonly expressed in mature neurons [52–54]. Collectively, the neuron-specific expression of MAP2 supports our results because the neuro-differentiated cells expressed vimentin, β3-tubulin, and SOX2, but showed weak MAP2 expression, which might indicate the immaturity of these differentiated cells.

Additionally, cumulus cells showed considerable spontaneous differentiation (Fig. 5). This might reflect the stemness criteria and may vary according to animal age, previous health condition, or the

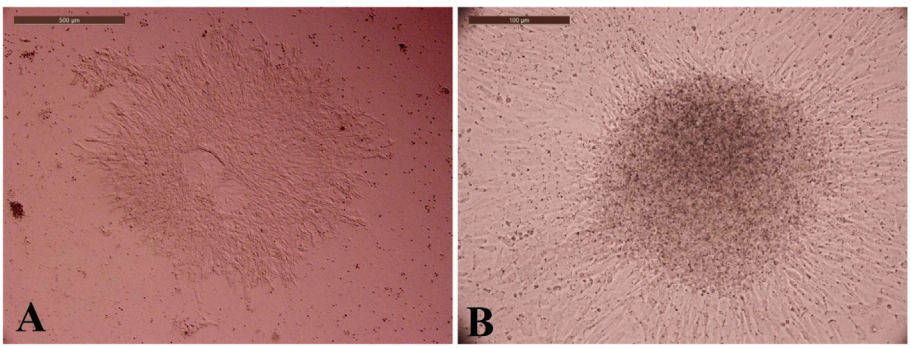

Fig. 7. Single cell culture of cumulus cells. During the micromanipulation of COCs, few cells (less than 10 cells) were detached from the holding pipette by hydraulic suction and cultured individually in four-well dishes. a. Cells showed rapid growth and colony formation (b), reached confluence after 7 days of culture (mean diameter of the colony = 4.2 ± 0.7 mm), and fully covered the surface area of the four-well dish (diameter is 1 cm) on day 10 of culture.

expression of reasonable amounts of other pluripotency markers (*POU5A1*, *KLF4*, *SOX2*, and *MYC*). Most importantly, this might reflect the existence of either very small embryonic-like (VSELs) cells, which was confirmed recently [37], or epithelial cells with multipotency criteria [17] that have spontaneous differentiation capabilities (reviewed in Refs. [16,55]). Moreover, granulosa stem cells survived when transplanted into immunodeficient mice and formed tissues of mesenchymal origin [11]. Interestingly, putative ovarian stem cells isolated from ovarian epithelium formed colonies consisting of different types of cells, including a small proportion of cells expressing certain markers of pluripotency [39,40], which agree with our results.

The paracrine or juxtacrine modes of communication with oocytes and the transcriptomes and endocrine functions of mural and cumulus granulosa cells vary even though both are derived granulosa cells [56–60]. Moreover, cumulus cells behave differently from mural granulosa cells in their response to gonadotrophins and the IGF-I analogue [61]. Additionally, follicular fluid aspiration may injure the follicular wall layers and result in mixed cell types such as theca or cumulus together with mural granulosa cells in the contents of aspirated follicular fluid. Hence, we used cumulus cells to confirm the selection of one type of cells in this current study.

Interestingly, the oocyte showed no effect on growth and differentiation or plasticity of the cumulus cells. This raises a question: how did the cumulus cells acquire stemness? There are two hypotheses; first, it might originate from the mesonephros or from the cycling progenitor cells on the surface epithelium of the ovary, at least throughout the initial waves of follicle formation after germ cell migration during embryogenesis [10,14]. Alternatively, the stemness-related transcripts might be acquired through the gap junctions and juxtacrine communication with oocytes in the earlier follicular development. Connexins mediate cell-to-cell transfer of mRNAs and short interfering RNAs by gap junctions [62–65]. Other studies showed that cumulus cells themselves or their conditioned medium are potent enhancers of pluripotent stem cell growth, which indicates a positive cross-talk between pluripotent cells and the cumulus cells and supports our hypothesis [66,67].

Our results, together with the findings from other studies, support the involvement of cumulus cells in the pathogenesis of ovarian diseases associated with metaplasia and transdifferentiation, such as ovarian osseous metaplasia and ovarian adipoma [10,11,15,21,23].

5. Conclusions

The discovery that cumulus cells possess exceptional plasticity among somatic ovarian cells definitely demands attention. Our results show that cumulus cells from COCs that are routinely discarded during the *in vitro* embryo production program might be an interesting subject to be researched and used in regenerative medicine in the future. Moreover, the current results provide a potential model for studying transdifferentiation in mammalian ovary, which is still poorly understood, thereby making cumulus cells interesting from the perspective of both human and veterinary medicine.

Disclosure statement

The authors declare that they have no competing interests.

Acknowledgements

The authors extend their appreciation to the Deanship of Scientific Research at King Saud University for funding this work through research group RG-1438-018.

Appendix A. Supplementary data

Supplementary data related to this article can be found at https://doi.org/10.1016/j.theriogenology.2018.06.009.

References

[1] Schmidt-Nielsen K. The physiology of the camel. Sci Am 1959;201:140–51.
[2] FAO, FAOSTAT. Live animals. 2013. http://wwwfaoorg/faostat/en/#data/QA.
[3] Gahlot T, Chouhan D. Fractures in dromedary (Camelus dromedarius)–A retrospective study. J Camel Pract Res 1994;1:9–14.
[4] Mohamed AF. Fractures in single-humped camels: a retrospective study of 220 cases (2008-2009). JKAU: Met Env Arid Land Agric Sci 2012;23:3–17.
[5] Hayashi K, Ochiai-Shino H, Shiga T, Onodera S, Saito A, Shibahara T, et al. Transplantation of human-induced pluripotent stem cells carried by self-assembling peptide nanofiber hydrogel improves bone regeneration in rat calvarial bone defects. Bdj Open 2016;2:15007.
[6] Sheyn D, Ben-David S, Shapiro G, De Mel S, Bez M, Ornelas L, et al. Human induced pluripotent stem cells differentiate into functional mesenchymal stem cells and repair bone defects. Stem Cells Transl Med 2016;5:1447–60.
[7] Hong So G, Winkler T, Wu C, Guo V, Pittaluga S, Nicolae A, et al. Path to the clinic: assessment of iPSC-based cell therapies in vivo in a nonhuman primate model. Cell Rep 2014;7:1298–309.
[8] Mohammadi-Sangcheshmeh A, Shafiee A, Seyedjafari E, Dinarvand P, Toghdory A, Bagherizadeh I, et al. Isolation, characterization, and mesodermic differentiation of stem cells from adipose tissue of camel (Camelus dromedarius). In Vitro Cell Dev Biol Anim 2013;49:147–54.
[9] Saadeldin IM, Swelum AA-A, Elsafadi M, Moumen AF, Alzahrani FA, Mahmood A, et al. Isolation and characterization of the trophectoderm from the Arabian camel (Camelus dromedarius). Placenta 2017;57:113–22.
[10] Kossowska-Tomaszczuk K, De Geyter C. Cells with stem cell characteristics in somatic compartments of the ovary. BioMed Res Int 2013;2013:1–8.
[11] Kossowska-Tomaszczuk K, De Geyter C, De Geyter M, Martin I, Holzgreve W, Scherberich A, et al. The multipotency of luteinizing granulosa cells collected from mature ovarian follicles. Stem Cell 2009;27:210–9.
[12] Riva F, Omes C, Bassani R, Nappi RE, Mazzini G, Icaro Cornaglia A, et al. In-vitro culture system for mesenchymal progenitor cells derived from waste human ovarian follicular fluid. Reprod Biomed Online 2014;29:457–69.
[13] Dzafic E, Stimpfel M, Virant-Klun I. Plasticity of granulosa cells: on the crossroad of stemness and transdifferentiation potential. J Assist Reprod Genet 2013;30:1255–61.
[14] Truman AM, Tilly JL, Woods DC. Ovarian regeneration: the potential for stem cell contribution in the postnatal ovary to sustained endocrine function. Mol Cell Endocrinol 2017;445:74–84.
[15] Varras M, Griva T, Kalles V, Akrivis C, Paparisteidis N. Markers of stem cells in human ovarian granulosa cells: is there a clinical significance in ART? J Ovarian Res 2012;5:36.
[16] Virant-Klun I, Stimpfel M, Skutella T. Stem cells in adult human ovaries: from female fertility to ovarian cancer. Curr Pharmaceut Des 2012;18:283–92.
[17] Lai D, Xu M, Zhang Q, Chen Y, Li T, Wang Q, et al. Identification and characterization of epithelial cells derived from human ovarian follicular fluid. Stem Cell Res Ther 2015;6.
[18] Dzafic E, Stimpfel M, Novakovic S, Cerkovnik P, Virant-Klun I. Expression of mesenchymal stem cells-related genes and plasticity of aspirated follicular cells obtained from infertile women. BioMed Res Int 2014;2014:508216.
[19] Brevini TA, Pennarossa G, Rahman MM, Paffoni A, Antonini S, Ragni G, et al. Morphological and molecular changes of human granulosa cells exposed to 5-azacytidine and addressed toward muscular differentiation. Stem Cell Rev 2014;10:633–42.
[20] Godbole P, Outram A, Sebire N. Osseous metaplasia in a benign ovarian cyst in association with cloacal anomaly. J Clin Pathol 2005;58:334–5.
[21] Miliaras D, Ketikidou M, Pervana S. Osseous metaplasia in ovarian tumours: a case with serous cystadenoma. J Clin Pathol 2007;60:582–3.
[22] Mukonoweshuro P, Oriowolo A. Stromal osseous metaplasia in a low-grade ovarian adenocarcinoma. Gynecol Oncol 2005;99:222–4.
[23] Akbulut M, Zekioglu O, Terek M, Özdemir N. Lipoma of the ovary: a case report and review of the literature. Ege J Med 2007;46:105–6.
[24] Zwiesler D, Lewis SR, Choo YC, Martens MG. A case report of an ovarian lipoma. South Med J 2008;101:205–7.
[25] Saadeldin IM, Swelum AA-A, Yaqoob SH, Alowaimer AN. Morphometric assessment of in vitro matured dromedary camel oocytes determines the developmental competence after parthenogenetic activation. Theriogenology 2017;95:141–8.
[26] Yaqoob SH, Saadeldin IM, Swelum AA-A, Alowaimer AN. Optimizing camel (Camelus dromedarius) oocytes in vitro maturation and early embryo culture after parthenogenetic activation. Small Rumin Res 2017;153:81–6.
[27] Saadeldin IM, Kim SJ, Lee BC. Blastomeres aggregation as an efficient alternative for trophoblast culture from porcine parthenogenetic embryos. Dev Growth Differ 2015;57:362–8.
[28] Schmittgen TD, Livak KJ. Analyzing real-time PCR data by the comparative CT method. Nat Protoc 2008;3:1101–8.
[29] Lin Y. Embryoid body formation from human pluripotent stem cells in chemically defined E8 media. StemBook 2014. https://www.ncbi.nlm.nih.gov/

books/NBK424234/. PMID 28211653.
[30] Elsafadi M, Manikandan M, Atteya M, Abu Dawud R, Almalki S, Ali Kaimkhani Z, et al. SERPINB2 is a novel TGFbeta-responsive lineage fate determinant of human bone marrow stromal cells. Sci Rep 2017;7:10797.
[31] Elsafadi M, Manikandan M, Alajez NM, Hamam R, Dawud RA, Aldahmash A, et al. MicroRNA-4739 regulates osteogenic and adipocytic differentiation of immortalized human bone marrow stromal cells via targeting LRP3. Stem Cell Res 2017;20:94–104.
[32] Deane CAS, Brown IR. Differential targeting of Hsp70 heat shock proteins HSPA6 and HSPA1A with components of a protein disaggregation/refolding machine in differentiated human neuronal cells following thermal stress. Front Neurosci 2017:11.
[33] Roy S, Gascard P, Dumont N, Zhao J, Pan D, Petrie S, et al. Rare somatic cells from human breast tissue exhibit extensive lineage plasticity. Proc Natl Acad Sci 2013;110:4598–603.
[34] Engler AJ, Sen S, Sweeney HL, Discher DE. Matrix elasticity directs stem cell lineage specification. Cell 2006;126:677–89.
[35] Schmidt EV. The role of c-myc in cellular growth control. Oncogene 1999;18:2988–96.
[36] Hurlin PJ, Dezfouli S. Functions of myc:max in the control of cell proliferation and tumorigenesis. Int Rev Cytol 2004;238:183–226.
[37] Parte S, Bhartiya D, Patel H, Daithankar V, Chauhan A, Zaveri K, et al. Dynamics associated with spontaneous differentiation of ovarian stem cells in vitro. J Ovarian Res 2014;7:25.
[38] Parte S, Bhartiya D, Telang J, Daithankar V, Salvi V, Zaveri K, et al. Detection, characterization, and spontaneous differentiation in vitro of very small embryonic-like putative stem cells in adult mammalian ovary. Stem Cell Dev 2011;20:1451–64.
[39] Virant-Klun I, Zech N, Rozman P, Vogler A, Cvjeticanin B, Klemenc P, et al. Putative stem cells with an embryonic character isolated from the ovarian surface epithelium of women with no naturally present follicles and oocytes. Differentiation 2008;76:843–56.
[40] Virant-Klun I, Rozman P, Cvjeticanin B, Vrtacnik-Bokal E, Novakovic S, Rulicke T, et al. Parthenogenetic embryo-like structures in the human ovarian surface epithelium cell culture in postmenopausal women with no naturally present follicles and oocytes. Stem Cell Dev 2009;18:137–49.
[41] Oki Y, Ono H, Motohashi T, Sugiura N, Nobusue H, Kano K. Dedifferentiated follicular granulosa cells derived from pig ovary can transdifferentiate into osteoblasts. Biochem J 2012;447:239–48.
[42] Mattioli M, Gloria A, Turriani M, Berardinelli P, Russo V, Nardinocchi D, et al. Osteo-regenerative potential of ovarian granulosa cells: an in vitro and in vivo study. Theriogenology 2012;77:1425–37.
[43] Mayerhofer A, Kunz L, Krieger A, Proskocil B, Spindel E, Amsterdam A, et al. FSH regulates acetycholine production by ovarian granulosa cells. Reprod Biol Endocrinol 2006;4:37.
[44] Mayerhofer A, Fritz S. Ovarian acetylcholine and muscarinic receptors: hints of a novel intrinsic ovarian regulatory system. Microsc Res Tech 2002;59:503–8.
[45] Schnitzer J, Franke WW, Schachner M. Immunocytochemical demonstration of vimentin in astrocytes and ependymal cells of developing and adult mouse nervous system. J Cell Biol 1981;90:435–47.
[46] Kriegstein A, Alvarez-Buylla A. The glial nature of embryonic and adult neural stem cells. Annu Rev Neurosci 2009;32:149–84.
[47] Lamouille S, Xu J, Derynck R. Molecular mechanisms of epithelial-mesenchymal transition. Nat Rev Mol Cell Biol 2014;15:178–96.
[48] Menezes JR, Luskin MB. Expression of neuron-specific tubulin defines a novel population in the proliferative layers of the developing telencephalon. J Neurosci 1994;14:5399–416.
[49] Katsetos CD, Karkavelas G, Herman MM, Vinores SA, Provencio J, Spano AJ, et al. Class III beta-tubulin isotype (beta III) in the adrenal medulla: I. Localization in the developing human adrenal medulla. Anat Rec 1998;250:335–43.
[50] Papanayotou C, Mey A, Birot AM, Saka Y, Boast S, Smith JC, et al. A mechanism regulating the onset of Sox2 expression in the embryonic neural plate. PLoS Biol 2008;6:e2.
[51] Zhang S. Sox2, a key factor in the regulation of pluripotency and neural differentiation. World J Stem Cell 2014;6:305.
[52] Soltani MH, Pichardo R, Song Z, Sangha N, Camacho F, Satyamoorthy K, et al. Microtubule-associated protein 2, a marker of neuronal differentiation, induces mitotic defects, inhibits growth of melanoma cells, and predicts metastatic potential of cutaneous melanoma. Am J Pathol 2005;166:1841–50.
[53] Tanapat P. Neuronal cell markers. Mater Methods 2013;3:196.
[54] Cavallaro M, Mariani J, Lancini C, Latorre E, Caccia R, Gullo F, et al. Impaired generation of mature neurons by neural stem cells from hypomorphic Sox2 mutants. Development 2008;135:541–57.
[55] Kranc W, Budna J, Dudek M, Bryja A, Chachula A, Ciesiolka S, et al. The origin, in vitro differentiation, and stemness specificity of progenitor cells. J Biol Regul Homeost Agents 2017;31:365–9.
[56] Saadeldin IM, Elsayed A, Kim SJ, Moon JH, Lee BC. A spatial model showing differences between juxtacrine and paracrine mutual oocyte-granulosa cells interactions. Indian J Exp Biol 2015;53:75–81.
[57] Diaz FJ, Wigglesworth K, Eppig JJ. Oocytes determine cumulus cell lineage in mouse ovarian follicles. J Cell Sci 2007;120:1330–40.
[58] Huang Z, Wells D. The human oocyte and cumulus cells relationship: new insights from the cumulus cell transcriptome. MHR: Basic Sci Reprod Med 2010;16:715–25.
[59] Chronowska E. High-throughput analysis of ovarian granulosa cell transcriptome. BioMed Res Int 2014;2014:1–7.
[60] Wigglesworth K, Lee K-B, Emori C, Sugiura K, Eppig JJ. Transcriptomic diversification of developing cumulus and mural granulosa cells in mouse ovarian Follicles 1. Biol Reprod 2015;92.
[61] Khamsi F, Roberge S. Granulosa cells of the cumulus oophorus are different from mural granulosa cells in their response to gonadotrophins and IGF-I. J Endocrinol 2001;170:565–73.
[62] Valiunas V, Polosina YY, Miller H, Potapova IA, Valiuniene L, Doronin S, et al. Connexin-specific cell-to-cell transfer of short interfering RNA by gap junctions. J Physiol 2005;568:459–68.
[63] Macaulay AD, Gilbert I, Scantland S, Fournier E, Ashkar F, Bastien A, et al. Cumulus cell transcripts transit to the bovine oocyte in preparation for Maturation 1. Biol Reprod 2016:94.
[64] Macaulay AD, Gilbert I, Caballero J, Barreto R, Fournier E, Tossou P, et al. The gametic synapse: RNA transfer to the bovine Oocyte 1. Biol Reprod 2014:91.
[65] Russell DL, Gilchrist RB, Brown HM, Thompson JG. Bidirectional communication between cumulus cells and the oocyte: old hands and new players? Theriogenology 2016;86:62–8.
[66] Assou S, Pourret E, Péquignot M, Rigau V, Kalatzis V, Aït-Ahmed O, et al. Cultured cells from the human oocyte cumulus niche are efficient feeders to propagate pluripotent stem cells. Stem Cell Dev 2015;24:2317–27.
[67] Shah SM, Saini N, Ashraf S, Singh MK, Manik RS, Singla SK, et al. Cumulus cell-conditioned medium supports embryonic stem cell differentiation to germ cell-like cells. Reprod Fertil Dev 2017;29:679.